[Frontiers in Bioscience 7, c97-110, September 1, 2002]

METHODS FOR STUDY OF PROTEIN DYNAMICS AND PROTEIN-PROTEIN INTERACTION IN PROTEIN-UBIQUITINATION BY ELECTRON PARAMAGNETIC RESONANCE SPECTROSCOPY

Heinz-Jürgen Steinhoff

Fachbereich Physik, Universität Osnabrück, Barbarastrasse 7, D-49069 Osnabrück, Germany

TABLE OF CONTENTS

1. ABSTRACT

Ubiquitination is a post-translation modification whereby the C-terminal end of ubiquitin (Ub) is covalently attached to the amino group of a lysine in a target protein. Additional ubiquitin groups are added using Ub-Ub linkages to form a polyubiquitin chain. A 26S protease complex specifically binds polyubiquitinated proteins and degrades them in an ATP-dependent manner. The target lysine in the substrate protein resides in a domain that is recognized by the ubiquitination machinery in a temporally and spatially controlled manner. The accessibility and the molecular dynamics of the target domain for each protein substrate is expected to be distinctive and this article is intended to facilitate investigations in this uncharted research area of ubiquitination mediated protein turnover by means of site-directed spin labeling. Examples illustrate the methodology of electron paramagnetic resonance data acquisition and interpretation in terms of secondary and tertiary structure resolution of proteins and protein complexes. Analysis of the spin labeled side chain mobility, its solvent accessibility, the polarity of the spin label micro-environment and distances between spin labels allow to model protein domains or protein-protein interaction sites and their conformational changes with a spatial resolution at the level of the backbone fold. The structural changes accompanying protein function or protein-protein interaction can be monitored in the millisecond time range. These features make site-directed spin labeling an attractive approach for the study of protein - ubiquitin interaction and protein ubiquitination.

2. INTRODUCTION

EPR spectroscopy of site-directed spin labeled biomolecules (*s*ite-*d*irected spin *l*abeling, SDSL) has emerged as a powerful method for studying the structure and conformational dynamics of proteins and nucleic acids under conditions relevant to function (for reviews see, e.g., (1-4)). In this technique, a spin label side chain is introduced at a selected site via cysteine substitution mutagenesis followed by modification of the unique

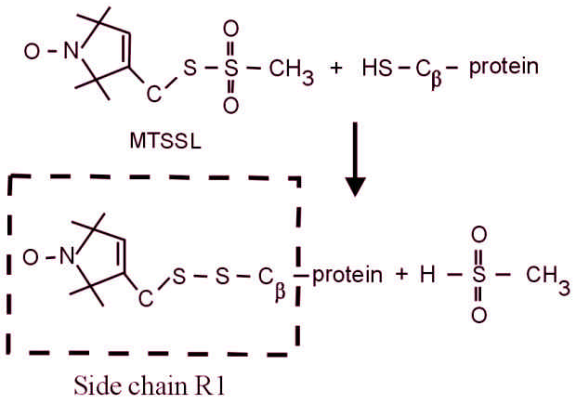

Figure 1. The reaction of the methanethio-sulfonate spin label with a sulfhydryl group, generating the spin label side chain R1.

sulfhydryl group with a specific paramagnetic nitroxide reagent. The continuous wave (cw) EPR spectrum yields information about the nitroxide side chain mobility, the solvent accessibility, the polarity for its immediate environment, and the distance between the nitroxide and another paramagnetic center in the protein. Hence, the EPR data analysis of a series of spin labeled variants of a given protein allows to define elements of secondary structure, including their solvent exposure, to characterize protein topography and to determine orientations of individual segments of the protein. The complete analysis allows modeling of protein structures with a spatial resolution at the level of the backbone fold (2, 3, 5-8). This method is applicable to any protein with a cloned gene that can be expressed. In particular, it has been shown to be very useful in studying large membrane proteins or protein complexes that are not amenable to NMR methods or do not crystallize. One of the most powerful properties of the method is its sensitivity to molecular dynamics: protein equilibrium fluctuations and conformational changes of functional relevance can be followed on a wide time scale ranging from picoseconds to seconds.

These features make SDSL a promising approach for the study of conformational dynamics involved in protein-protein interaction including the investigation of protein ubiquitination. In the post-translational modification process of ubiquitination the C-terminal end of ubiquitin is attached covalently to a lysine residue on the target protein substrates. Additional ubiquitin groups are added using Ub-Ub linkages to form a poly-ubiquitin chain. A 26S protease complex specifically binds poly-ubiquitinated proteins and degrades them in an ATP-dependent manner (9 - 11). The recognition determinants for ubiquitination do not have a motif, vary in complexity, and the rates of ubiquitination are also dependent on conformational changes and dynamics of the target domains in the case of individual proteins. Also, different domains of a protein may be targeted for ubiquitination under different conditions (reviewed in (14)). For example, cytochrome P450 2E1 (CYP2E1) levels are elevated in response to substrates such as ethanol, and it has been postulated that substrate binding alters the conformational states and dynamics of the ubiquitination target domains on the CYP2E1 protein (12-14). The substrate recognition phenomenon remains complex and very little, if any, investigation has been undertaken to elucidate the dynamic states of the target domain of a protein undergoing ubiquitination.

The present article summarizes recent progress of the SDSL methodological approach with special emphasis on possible application to the study of molecular dynamics and protein-protein interaction in protein-ubiquitination.

3. SAMPLE PREPARATION

Cysteine residues may be modified with a variety of nitroxides to yield a spin label side chain. However, the methanethiosulfonate spin label (1-oxyl-2,2,5,5-tetramethylpyrroline-3-methyl)methanethiosulfonate (MTSSL) ((15); TRC, Toronto) is most often used in SDSL studies due to its sulfhydryl-specificity and its small molecular volume, similar to the phenylalanine or tryptophane side chains (figure 1). In addition, the unique dynamic properties of this spin label side chain facilitates detailed structural information determined from the shape of its EPR spectrum (see section 4.1). A general scheme of the spin labeling procedure proven to yield good labeling efficiency is as follows: After cysteine-substitution mutagenesis the purified protein is usually stored in the presence of DTT in order to prevent oxidation of the cysteine. Before spin labeling the protein solution has to be dialyzed against 100 mM sodium phosphate buffer, pH 7.0 to dilute the concentration of DTT. The protein (concentration adjusted to, e.g., 20 μM) is then incubated with 100 μM spin label at 4°C for 12 hours. The unbound spin label is removed by gel filtration using Sephadex G-25 mini columns from Pharmacia (Freiburg, FRG). The spin labeled protein is concentrated to between 10 and 100 μM and filled into EPR quartz capillaries. At X-band (microwave frequency 9.5 GHz, magnetic field 0.34 T), the use of loop gap or dielectric resonators provide the necessary sensitivity to yield continuous wave EPR spectra with good signal to noise ratio using 5 μL of sample within scan times of between 5 and 30 minutes. The spin labeled cysteine/protein ratio is determined by double integration of the EPR spectra followed by comparison with standard solutions of (1-oxyl-2,2,5,5-tetramethylpyrroline-3-methyl)methanethiosulfonate and determination of the protein concentration. For inter-spin distance measurements (see section 4.5) this ratio has to be close to one. To assure selective spin labeling accessible native cysteines have to be replaced by serines or alanines. The integrity of the spin labeled protein variants has to be checked using independent methods.

4. STRUCTURAL INFORMATION DERIVED FROM EPR SPECTRA ANALYSIS

4.1. Nitroxide dynamics and motional freedom

The sensitivity of the EPR spectra to the reorientational motion of the nitroxide side chain has been extensively reviewed (16-18) and the relationship between

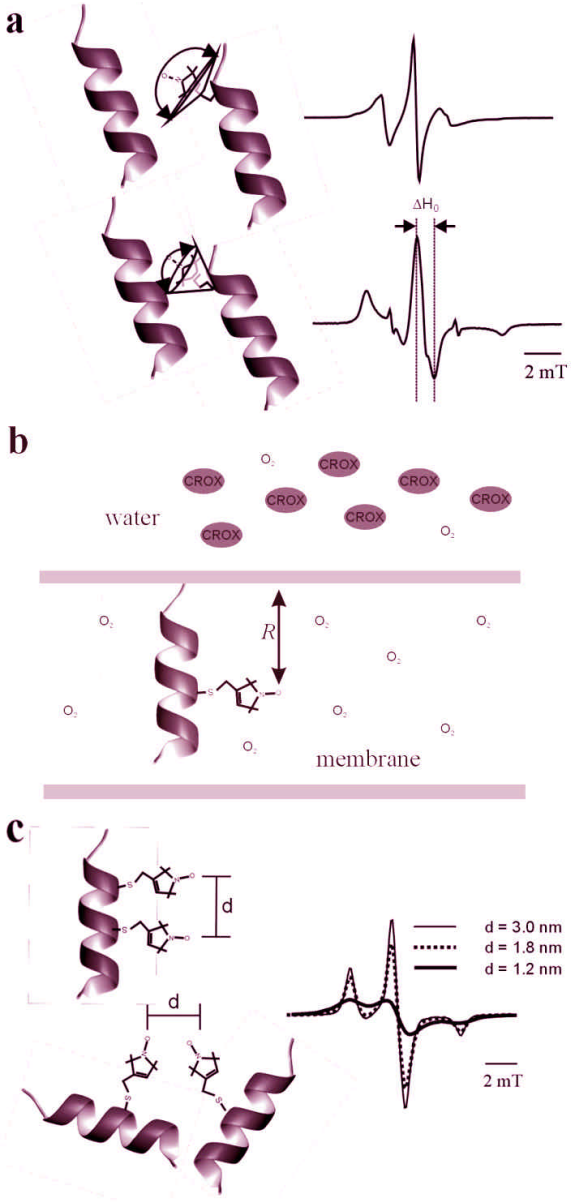

Figure 2. (a) Tertiary structural elements with low (top) and high (bottom) restriction of the spin label side chain mobility due to interaction with the neighboring backbone. Room temperature (T = 293 K) X-band (9.5 GHz, 0.33T) EPR spectra depicted in the usual 1st derivative representation show the typical shape for the respective site: the anisotropy of the hyperfine interaction is partially averaged due to the spin label motion (top), whereas a powder like spectrum results in the case of restricted motion (bottom). The total scan range for all spectra shown is 12.8 mT. (b) The collision frequency of a membrane inserted spin label side chain with paramagnetic quenchers of different solubility in the lipid and aqueous phases, e.g. chromium oxalate (CROX) and molecular oxygen, is measured by continuous wave (cw) EPR saturation techniques and provides the distance R between the nitroxide and the water-lipid interface of the membrane. (c) Evaluation of the inter-spin distance between two bound spin label side chains allows determination of secondary (top) and tertiary (bottom) structural elements. Simulated X-band EPR spectra (T = 170 K, normalized to constant spin number) are shown on the right demonstrating the increase of the spectral line width (dipolar broadening) with decreasing inter-spin distance.

side chain mobility and protein structure has been explored in detail for T4 lysozyme (19). The term "mobility" is used in a general sense and includes effects due to the motional rate, amplitude and geometry. The degree of motional restriction of the nitroxide side chain depends on the secondary and tertiary structure of the spin label binding site and its micro-environment. Weak interaction between the nitroxide and the rest of the protein as found for helix surface sites or loop regions results in a high degree of mobility. In this case the apparent hyperfine splitting and the line width are as small as illustrated in figure 2a. In turn, if the residual motion is restricted due to strong interaction of the nitroxide group with neighboring side chains or backbone atoms as found for tertiary contact or buried sites, the apparent hyperfine splitting and the line width are increased. In general, the resulting spectra cannot be simulated with a simple isotropic model of motion. Due to the interaction of the nitroxide with neighboring protein atoms the motion has to be anisotropic as was shown by molecular dynamics simulations (20, 21). Additionally, a distribution of motional states can be concluded from those spectra which exhibit more than one component. In spite of this complicated nature of the nitroxide dynamics a simple semi-empirical mobility parameter, the inverse line width of the center line, Delta H_o^{-1}, determined by the degree of averaging of the anisotropic g and hyperfine tensors, has been found to be correlated with the structure of the binding site environment (1, 19, 22). It has been shown that the plot of this parameter versus residue number reveals secondary structure through the periodic variation in mobility as the nitroxide sequentially samples surface, tertiary or buried sites. The assignment of alpha-helices and beta-strands from the data is straightforward.

The strategy for detecting and interpreting the experimental data are illustrated with examples of structural details in bacteriorhodopsin (BR). BR is a light driven pump which translocates protons across the cell membrane of the archaebacterium *Halobacterium salinarum*. Figure 3a shows the structure determined by x-ray diffraction. It consists of seven transmembrane helices which bury the chromophore retinal (23). The structure of the E-F loop was found to be only poorly resolved in several of the reported x-ray diffraction experiments most probably due to structural disorder or its high flexibility (24-26). The EPR spectra and the values of the inverse line width of the center line, Delta H_o^{-1}, for the spin labeled E-F loop sites and for the cytoplasmic end of helix F, positions 160 to 171, are shown in figure 3b and 3d (27). The mobility of the spin label side chains attached to positions 161, 162 164, 165 and 166 are only slightly restricted which is evidence for an orientation with small tertiary interaction. The reorientational motion of the nitroxides attached to 167 and 168 is strongly restricted by interaction with helices C and E, respectively. The side chain at position 169 could be shown to be in contact with a BR molecule of a neighboring trimer. Positions 170 and 171 provide locations of the nitroxide already in the interior of the protein. Restricted motion dominates the spectra of A160R1 and M163R1. This is strong evidence for a loop conformation with these two nitroxide side chain oriented

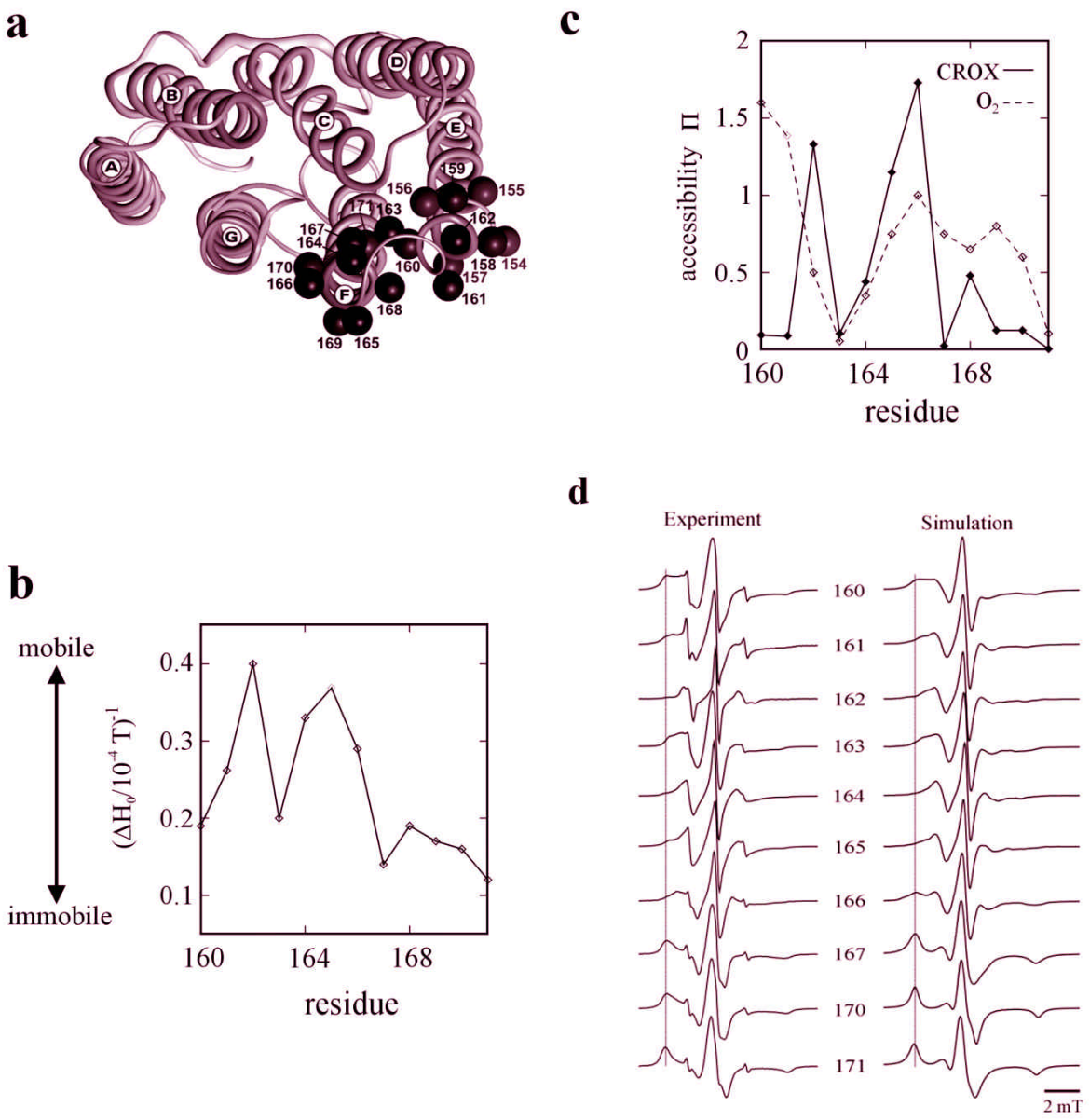

Figure 3. (a) The backbone structure of bacteriorhodopsin (BR) (23). The seven transmembrane helices, which are denoted A through G, are shown from the cytoplasmic side. The indicated residues in the E-F loop and in the cytoplasmic end of helix F were exchanged by cysteines one by one and spin labeled with MTSSL. (b) The inverse line width of the center line of the EPR spectra shown in (d) plotted versus position of the spin label in the BR sequence from 160 to 171 (27). The inverse line width is a measure of the spin label side chain mobility. Small values represent immobile side chains due to strong interactions of the nitroxide with neighboring protein atoms, high values represent a mobile spin label side chain. (c) The accessibility parameter for chromium oxalate (solid line, filled symbols) or oxygen (dashed line, open symbols) versus sequence number. PI_{oxygen} was determined in equilibrium with air and scaled to pure oxygen, PI_{CROX} was measured in the presence of 50 mM CROX (27). (d) *Left column:* Experimental EPR spectra (1^{st} derivative, T = 293 K, 9.5 GHz) of BR mutants spin labeled at positions 160 through 171. The vertical line indicates the position of the low field hyperfine extreme that characterizes immobilized nitroxides. *Right column:* EPR spectral simulations based on molecular dynamic trajectories according to the methods described (20, 21).

towards the protein. The arrangement of the residues 160 to 165 within a single turned loop is one possibility which nicely agrees with the experimental data. This arrangement is consistent with the structure model obtained from X-ray diffraction data by Essen and coworkers (23) (figure 3a) and provides strong evidence that the loop structure found under physiological conditions is retained in the crystal state.

4.2. Molecular dynamics simulations and EPR spectra calculations

A more quantitative interpretation of the experimental data in terms of dynamic mechanisms and local tertiary interaction requires the simulation of EPR spectra. Simulations on the basis of dynamic models (28-30) show excellent agreement with the corresponding experimental spectra of solvated spin labels or spin labeled lipids and proteins and give very valuable insight in the dynamics of these systems. Furthermore, simulations of EPR spectra on the basis of molecular dynamics simulations facilitate the study of influence of the structure in the vicinity of the spin label binding site on the EPR spectral line shape (20, 21). This approach allows to verify, refine or suggest structural models on the basis of experimental EPR spectra of singly spin labeled proteins.

As an illustrative application of this approach data of the spin label side chains in the sequence from position 160 to 167 in the E-F loop, and positions 170 and 171 in the cytoplasmic end of helix F of BR is reviewed here (21). Molecular dynamics simulations of the spin labeled protein were performed with the atomic data taken from Essen *et al.* (23). The free energy surface of the spin label orientations calculated from each spin label side chain trajectory using the GROMOS (Biomos, Groningen) program package is the starting point of the simulation protocol by means of the program MDEPR (20). The comparison of the resulting simulated spectra with the experimental data shown in figure 3d reveals agreement of the spectral shapes and splitting for the whole sequence shown with the exception of position 166. Here, the simulated spectrum reveals a component of restricted motion which is not visible in the experimental spectrum. This most probably reflects the high flexibility of the last cytoplasmic turn of helix F under physiological conditions which is not accounted for in the molecular dynamic calculations, because the backbone atoms of the helices were restrained during the simulations. However, the motional restrictions due to tertiary interaction for positions 167, 170 and 171 are visible in the appearance of outer peaks in the low field and high field extremes of both the simulated and the experimental spectra (indicated by vertical bars in figure 3d). This proves the structural data of this sequence obtained for BR in the crystal state to be valid also under physiological conditions, *i.e.* inserted in the native membrane.

4.3. Solvent accessibility of the attached nitroxides

The motional analysis of elements of secondary and tertiary structure can be supplemented by measuring the collision frequency of the nitroxide side chains with freely diffusing paramagnetic probe molecules. The collision frequency of such a probe depends on the product of its translational diffusion coefficient and its local concentration. Molecular oxygen and the water soluble paramagnetic Ni(II) complexes or chromium oxalate (CROX) are frequently used and are ideally suited because of their sizes and solubility properties (31, 32). In a water/membrane system these molecules are partitioned between the water and the hydrophobic phase according to their polarity. Polar metal complexes preferentially partition into the aqueous phase, whereas the product of concentration and diffusion coefficient of apolar oxygen has been shown to increase with the distance from the membrane/water interface and exhibits a maximum value in the center of the membrane bilayer (figure 2b) (33). Hence, determination of the collision frequency of nitroxide side chains with these paramagnetic reagents in solution allows identification of the side chain orientations with respect to the protein-water or protein-lipid interface and its position relative to the membrane. The collision frequencies can be quantified by the method of continuous wave power saturation (33). For that purpose the samples are loaded into gas-permeable TPX capillaries (Spintec, Germany). The samples are deoxygenated by passing nitrogen around the sample capillary. For oxygen accessibility experiments, nitrogen is replaced by air. Saturation curves are determined from the peak-peak amplitudes of the center line measured at different incident microwave power levels. The saturation behavior of the samples is then parameterized by the quantity $P_{1/2}$, which is defined as the power level of the incident radiation at which the amplitude of the saturated line is half of the amplitude in absence of saturation. Values for this parameter are calculated from fitting of the function

$$A(P) = I\sqrt{P}\cdot(1+(2^{1/b}-1)\cdot P/P_{1/2})^{-b}$$

to the experimental amplitudes A(P) (33). The scaling factor, *I*, and the measure of the saturation homogeneity, *b*, are adjustable parameters. A quantity Delta $P_{1/2}$ is then calculated from the difference in $P_{1/2}$ values in the presence and absence of the of relaxing agent. The Delta $P_{1/2}$ values are divided by the peak-peak line width, Delta H_o, and normalized by the same quantities of a DPPH standard sample to obtain a dimensionless accessibility parameter PI, which is proportional to the collision frequency of the nitroxide with the respective reagent.

As an example the accessibility parameter values for the BR variants are depicted as a function of sequence position (figure 3c). The highest values of PI_{CROX} and hence the highest collision frequency with CROX is revealed for the side chains attached to positions 162, 164, 165, 166 and 168. These residues must be oriented towards the aqueous phase while those with low PI_{CROX} face the protein or the bilayer. The accessibility parameter PI_{oxygen} allows to discriminate between these two cases. Low oxygen accessibility is typical of the location of the nitroxide side chain buried inside the protein. High oxygen accessibility is characteristic of the nitroxide in contact with the lipid bilayer. The oxygen accessibility is lowest for positions 163 and 171. The nitroxide side chains attached to these positions must therefore be in the protein interior. The low accessibility for CROX for positions 160 and 161 is accompanied by very high collision frequencies with oxygen. Hence, this is evidence for a location of these nitroxide side chains with contact to the bilayer, where oxygen concentration is enhanced compared to the aqueous phase. Again, these findings are in agreement with the structure model.

Besides the valuable secondary and tertiary structure information extracted from the accessibility data it

has furthermore been shown that concentration profiles of oxygen and the polar Ni(II) complexes in a lipid bilayer can be used to measure the depth of the lipid exposed sites in a membrane (cf. figure 2b) (33).

4.4. Polarity of the nitroxide micro-environment

The development of high-field EPR techniques requiring super-conducting magnets has enhanced the Zeeman resolution of rigid-limit spectra of disordered samples from which the principal g-tensor components and their variation due to solute-solvent interactions can be determined with high accuracy (34-36). The sensitivity of W-band EPR (95 GHz, 3.4 T) to the matrix polarity in the vicinity of the spin label binding site allows to monitor the water density on the protein surface or within the interior of ion channels and its variation upon protein-protein interaction or conformational changes. Generally, a polar environment shifts the tensor component g_{xx} to smaller values whereas the tensor component A_{zz} is increased (37). In a sequence of a regular secondary structure with anisotropic solvation, the water density and hence the tensor component values are a periodic function of sequence number similarly to the behavior of the accessibility for water soluble paramagnetic ions (see section 4.3).

For the purpose of polarity analysis W-band EPR spectra have to be recorded at low temperatures to avoid motional averaging of the anisotropic tensors. In the temperature regime below 200 K the reorientational correlation time of an otherwise unrestricted spin label side chain exceeds 100 ns (38), i.e. the nitroxide may be considered as immobilized on the EPR time scale. Librational motion of small amplitude still prevails and may lead to small deviations of the measured tensor values from their rigid limit values due to partial motional averaging. However, this effect is small (e.g. less than 2% for A_{zz} at 200 K (38)) and is further minimized by decreasing the temperature for data collection to 120 K. Sample spectra of spin label side chain attached along the BR proton channel are shown in Figure 4. The variation of g_{xx} with the nitroxide binding site is revealed by the shift of the position of the low-field maximum. The plot of g_{xx} versus nitroxide position along the proton channel reveals distinct variations in the polarity of the nitroxide micro-environment. Residues S162R1 and M163R1 are located in the E-F loop at the cytoplasmic surface, whereas residue K129R1 is positioned in the D-E loop on the extracellular surface. The high polarity in the environment of these residues is clear evidence that the nitroxides are accessible to water, which is in agreement with the structure. The environmental polarity of the nitroxide at positions 100, 167 and 171 is significantly less and reaches its minimum at position 46 between the proton donor D96 and the retinal. The plot directly reflects the hydrophobic barrier, which the proton has to overcome on its way through the protein. The analysis of both tensor components, g_{xx} and A_{zz}, allows in addition the characterization of the micro-environment of the spin label side chain in terms of protic and aprotic (39). Furthermore, the polarity variation with bilayer depth across the lipid-exposed surface of a transmembrane alpha-helix can be used to locate a spin labeled site with respect to the lipid-water interface (Steinhoff and Wegener, unpublished) and provides valuable information on the orientation of membrane associated proteins or membrane anchors.

4.5. Inter-nitroxide distance measurement

Mobility, accessibility, and polarity analyses provides a unique means of deducing sequence-specific secondary structure in a protein. The simultaneous exchange of two native amino acids by cysteines followed by modification with methanthiosulfonate spin labels allows determination of inter-residual distances (for reviews see (40, 41)) and thus provides a strategy for deducing proximity of selected secondary structural elements.

The spin-spin interaction between two spin labels attached to a protein is composed of static dipolar interaction, modulation of the dipolar interaction by the residual motion of the spin label side chains and exchange interaction. The static dipolar interaction leads to considerable broadening of the cw EPR spectrum if the inter-spin distance is less than 2 nm. For unique orientations of the nitroxides relative to each other as found for spin labels introduced at buried sites in the rigid limit a rigorous solution of the spin Hamiltonian of the system can be obtained. Spectra simulations yield the distance between the nitroxides and the Euler angles describing their relative orientation and that of the inter-spin vector relative to the magnetic field (40, 42). However, the most frequently encountered case in SDSL consists of nitroxides that adopt a statistical distribution of distances and relative orientations. Values of the inter-spin distances can be determined from a detailed line shape analysis of spectra measured below 200 K (43-45) or in solutions of high viscosity (46) using spectra convolution or deconvolution techniques. The EPR spectra simulations program DIPFIT (43, 45), e.g., employs automated routines to determine best-fit parameters and considers a gaussian distribution of inter-spin distances and variable contributions of singly spin labeled protein. Since the line width of the spectra is a steep function of the inter-spin distance (see figure 2c), empirical or semi- empirical parameters as spectral amplitude ratios or spectral second moment values are often sufficient to answer structural questions (7, 47). The lower limit for reliable distance determination using the above methods is given by the increasing influence of exchange interaction with decreasing inter-spin distances due to partial overlap of the nitrogen π-orbitals of the two interacting nitroxides. This effect makes quantification of inter-spin distances of less than 0.8 nm difficult (48, 49). In particular, a simplified inter-spin distance determination using the difference of spectral second moments

$$\left\langle DeltaB_D^2 \right\rangle = \frac{\int (B - B_{FD})^2 S_D(B) dB}{\int S_D(B) dB} - \frac{\int (B - B_{FS})^2 S_S(B) dB}{\int S_S(B) dB}$$

does not depend on exchange interaction and is less sensitive to incomplete spin labeling in comparison to the analysis of spectral amplitude ratios. $S_D(B)$ is the absorption spectrum of the doubly spin labeled protein

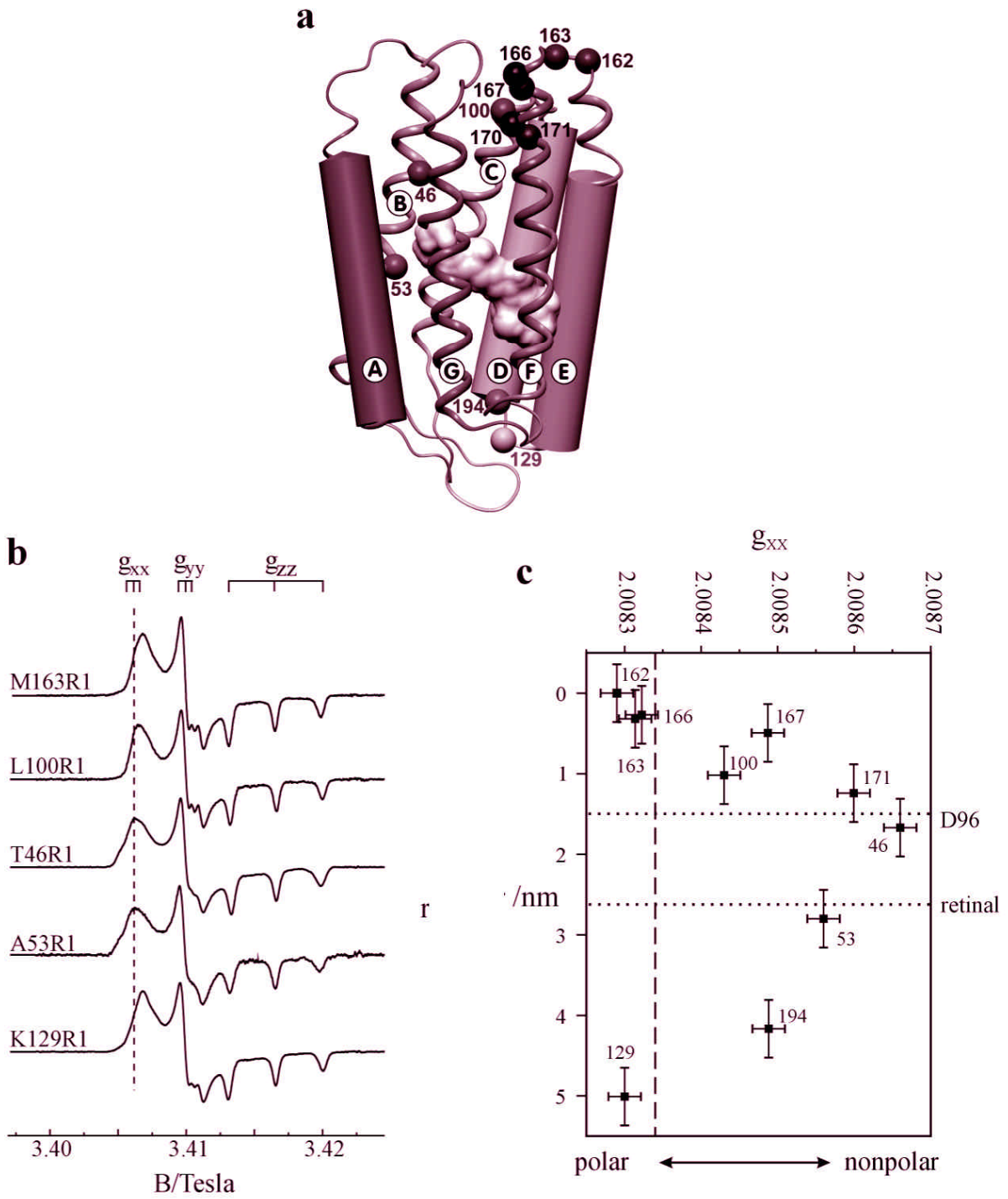

Figure 4. (a) Structure of bacteriorhodopsin (BR) with labeled C-alpha atoms of the spin labeled residues. (b) Experimental high-field EPR spectra (1st derivative, T = 200 K, 95 GHz) for a set of spin labeled BR variants. The hyperfine splitting in the g_{xx} and g_{yy} regions is not completely resolved. The vertical line marks the g_{xx} position of T46R1. The variation of g_{xx} reflects the change of polarity in the micro-environment of the spin label when moving through the BR proton channel from the cytoplasmic to the extracellular side. (c) The component g_{xx} of spin label side chains oriented to the aqueous phase or into the proton channel as a function of the nitroxide position, r, with respect to position 164. The broken line shows the g_{xx} value for unbound spin label, the dotted lines indicate the positions of the proton donor D96 and the retinal, respectively. The value of g_{xx} can be understood as a polarity index, thus the plotted data reflect the hydrophobic barrier in the BR proton channel (modified from (39)).

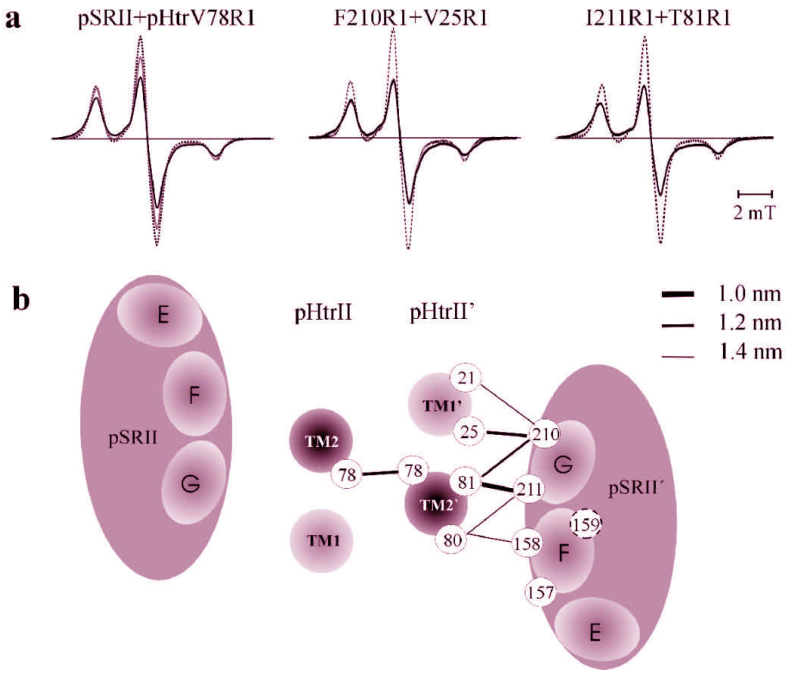

Figure 5. (a) EPR spectra (T = 170 K) of spin labeled mutants of the truncated transducer pHtrII in 1:1-complex with the receptor sensory rhodopsin pSRII or spin labeled pSRII mutants. All samples are reconstituted into purple membrane lipids. Spin normalized EPR powder spectra of the ground state (black) are compared with the M-accumulated state (gray) and reference spectra without dipolar broadening (dotted). The strength of dipolar interaction and the resulting line broadening is obvious by comparing the amplitudes of spin number normalized spectra of the reconstituted complexes with the reference samples. (b) Schematic model of the transmembrane region of the proposed 2:2-complex of pSRII with its transducer pHtrII (view from cytoplasm). The structural model of pSRII is based on a BR-crystal structure (23), validated for side chains 157-160 (F-helix) and 210-213 (G-helix) (74). Transmembrane helices of pHtrII are modeled as canonical alpha-helices, TM1 and TM2. These components are oriented with respect to each other based on dipolar spin-spin interactions and derived distance constraints. Strong dipolar interactions due to inter-spin distances less than 1.4 nm between spin labeled positions of pSRII and pHtrII or within the pHtrII dimmer (78-78) are coded by the thickness of connecting lines (8).

sample and $S_S(B)$ is the corresponding spectrum without spin-spin interaction determined from the superposition of the two corresponding singly spin labeled protein samples. B_{Fi} and B are the first spectral moments and the magnet field, respectively. In the case of a radical pair, the relation between the difference of second moments, $<Delta\ B^2_D>$, and the inter-spin distance, r, yields

$$r = 2.32 * <Delta\ B^2_D * 10^8>^{-1/6} \text{ nm},$$

with $<Delta\ B^2_D>$ given in T^2. The upper limit for distance determination using the method of second moments is between 1.5 and 1.7 nm depending strongly on the quality of the baseline. Convolution and deconvolution techniques were shown to be applicable for inter-nitroxide distances up to 2 nm and provide valuable information on distance distributions. Recent advance in pulsed EPR techniques leads to protocols which expand this range from 2 to 8 nm (50, 51). Hence, cw EPR and pulsed EPR methods perfectly complement each other and provide inter-spin distances in the range between 0.8 and 8 nm.

The method of inter-spin distance determination has been successfully applied to a number of proteins, including rhodopsin (52-54), lac permease (55), the KcsA potassium channel (6) and alpha-crystallin (5, 56). These applications demonstrate the capability and reliability of the SDSL method in resolving protein structure at the level of the backbone fold. In addition, changes in dipolar interaction can result in large spectral changes, making it straightforward to monitor conformational changes (57-59) (see also section 5).

As an example for the elucidation of protein-protein interaction using dipole-dipole interaction, the determination of a structural model of the membrane protein complex consisting of the sensory rhodopsin receptor pSRII and the transducer pHtrII is described (figure 5) (8). Inter-spin distances were obtained for 26 pairs of spin labels introduced into the transmembrane helices TM1 or TM2 of the transducer and helices F or G of the receptor. Considerable spin-spin interactions observed for the singly labeled transducer with the nitroxide side chain located at position 78 or 82 confirmed a dimeric arrangement of TM2 and TM2'. The strongest interaction corresponding to the closest distances (less than 1.2 nm) between pSRII and pHtrII are observed between positions 25^{TM1}-210^{G}, 81^{TM2}-210^{G}, as well as between 81^{TM2}-211^{G} indicating that both TM1 and TM2 are close to helix G. Distances in the range from 1.2 to 1.6 are determined for

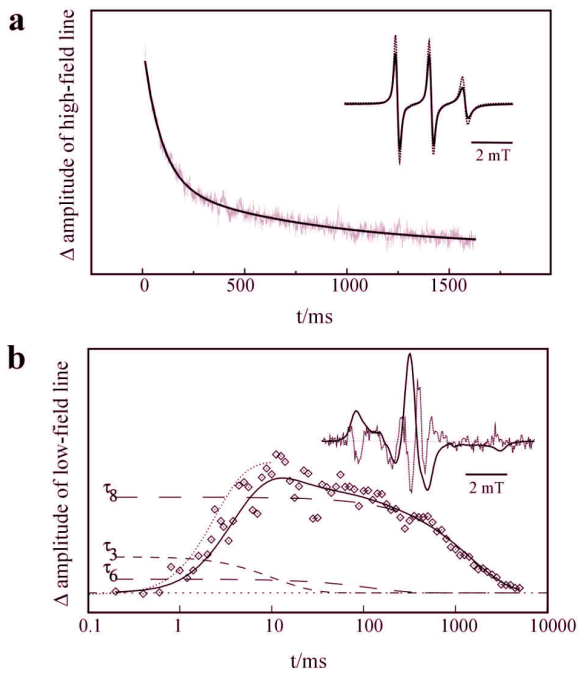

Figure 6. (a) Refolding of cytochrome c: Amplitude change of the EPR high-field peak of spin labeled cytochrome c after rapid dilution of the denaturant GuanidineHCl from 3.5 M (unfolded) to 1.75 M (folded). The continuous line shows a fitted bi-exponential function with time constants of 90ms and 800ms. The cw-spectra of the folded (continuous line) and unfolded states (dotted line) are shown in the inset. (b) Conformational changes of bacteriorhodopsin during the photocycle: EPR amplitude change of the low-field peak of F171R1 after photo-excitation (diamonds). Multi-exponential fit curve (full line) and the dominating time constants (τ_3, τ_6, τ_8), which contribute to the signal decay, are included (broken lines). The dotted line shows the behavior of the fast fraction of the M decay which was determined from measurements of the absorbance changes in the visible spectrum. The inset depicts the continuous-wave EPR spectrum and the kinetic difference spectrum (light minus dark, dotted line) of F171R1 (72). Spectra simulations of the difference spectrum and high-field EPR spectroscopy reveal a transient mobilization of the spin label side chain combined with a polarity change of the nitroxide environment (21, 75).

the following four TM2-pSRII pairs: 80^{TM2}-158^{F}, 80^{TM2}-157^{F}, 80^{TM2}-210^{G}, 80^{TM2}-211^{G}, and 81^{TM2}-158^{F}. According to these inter-spin distance values TM2 has to be located between the C-terminal helices F and G as depicted in figure 5. The specific dimer formation of the pSRII/pHtrII complex in membranes orients the respective positions 22 of TM1 and TM1' towards each other (not shown). These findings and the distance values determined between the residual spin labeled positions of TM1, 21, 23, 24, and 25 with 210 or 158 are in agreement with this arrangement (8). These results reveal a quaternary complex between two copies of pHtrII and pSRII each, forming a structure with an apparent two-fold symmetry (figure 5).

Metal ion - nitroxide interactions in metallo-proteins or engineered copper-ion-binding sites allow estimation of intramolecular distances also at room temperature (60, 61). A single metal ion provides a reference site for the estimation of distances to multiple nitroxide sites and first applications to proteins of unknown structure have been reported (62).

5. TIME RESOLVED DETECTION OF CONFORMATIONAL CHANGES

One attractive feature of site directed spin labeling is the ability to time resolve changes in any of the parameters discussed above. Hence, changes in the protein secondary structure, protein tertiary fold or domain movements can be followed with up to 100 μs resolution with conventional EPR instrumentation and detection scheme (field modulation). Important examples found in the literature include the detection of rigid body helix motion in both rhodopsin and bacteriorhodopsin (57, 63-66), domain movements in T4 lysozyme (1), structural reorganization in colicin E1 (67) upon membrane binding and conformational changes during signal transfer from sensory rhodopsin pSRII to the transducer pHtrII (8). The strategy for triggering, detecting and interpreting conformational changes are illustrated with examples of changes of the tertiary interaction in cytochrome c upon refolding and in bacteriorhodopsin upon photo-isomerization of the retinal. These experiments provide the timescale and location of conformational changes. In addition, time resolved detection of inter-spin distance changes reveal the magnitude of helix motion as will be demonstrated with the examples of bacteriorhodopsin and the sensory rhodopsin-transducer complex (8, 47).

5.1. Changes in tertiary interaction

As outlined in section 4.1 the shape of the nitroxide EPR spectra at room temperature is primarily determined by the tertiary interactions of the spin label side chain. As an example the spectra of folded and unfolded cytochorme c with a iodoacetamid spin label non selectively attached to accessible lysines is shown in figure 6a. Compared to the native conformation the mobility of the nitroxide side chain is significantly increased in the unfolded state due to minor tertiary interaction. After rapid dilution of the denaturant (GuanidineHCl), refolding of the protein can be followed by recording the time course of the EPR signal with the B-field fixed at values where the spectra of the folded and unfolded states show maximum difference. The data reveal at least a biphasic folding reaction with times constants of 90 and 600 ms depending on the final denaturant concentration (Kühn and Steinhoff, unpublished). The agreement with results of fluorescence and UV/VIS experiments (68) prove that the rearrangement of the protein surface structure occurs synchronously with the folding of the structure in the environment of the heme or tryptophane. Recent rapid-mix flow and stopped-flow kinetic EPR experiments on site-directed spin labeled yeast iso-1-cytochrome c show that this technique allows to observe folding reactions and conformational changes on a time scale stretching from about 50 μs to seconds (69).

If the protein conformations of interest are of transient nature the strategy to determine the properties of the respective intermediate EPR spectra includes the direct detection of kinetic difference spectra. This is best illustrated in the case of BR: difference spectra between the photo-activated state and the initial state of BR have been determined during a single B-field scan by subtraction of the signals averaged within two succeeding sampling intervals starting with the light flash. The lengths of the sampling intervals are set to values longer than the recovery time of the initial state (47, 64). Following this scheme the signal recorded during the first sampling interval is an average of the signals of all photo-intermediates including the initial state. The signal determined during the second sampling interval represents the recovered pure initial state. Upon activation of BR by a light flash conformational changes are reflected in transient changes of the EPR spectral line shape of the nitroxide side chains in the cytoplasmic loops and helix F (64, 70-72). As an example the difference spectra and the time course of the transient EPR signal change of the spin label side chain at position 171 are shown in figure 6b. A systematic investigation of a series of BR variants with spin label side chains introduced along the E-F loop and into the cytoplasmic ends of helices E and F provides evidence for a transient increase of the motional freedom for the side chains located between helices B, C and F and thus point towards a transient outward movement of helix F during the photocycle (72). The kinetics of this conformational change can be followed at fixed B-field values where the difference spectrum show local extremes. Time constants of the rise and decay of the intermediate with changed conformation are determined from a fitted superposition of exponentials. A comparison with the respective time constants for the photocycle intermediates of BR determined from optical and FTIR spectroscopy reveal that the observed conformational change occurs in phase or slightly prior to the reprotonation of the Schiff base depending on the nitroxide location (71, 72).

5.2. Detection of inter-spin distance changes

5.2.1. Bacteriorhodopsin – dynamic changes in the same protein

The magnitude of the conformational change can be determined from the inter-spin distances of stabilized intermediates. For stabilizing the M intermediate of BR the sample is cooled to 220 K prior to illumination. This protocol has been shown to accumulate the M intermediate to approximately 75% (47). The BR initial state spectrum of V101R1&A168R1 and the corresponding spectrum of the M intermediate are compared in figure 7. The BR initial state EPR spectrum shows broad lines due to spin-spin interaction which are pronounced in the low- and high-field regions. The line width is considerably reduced in the trapped M intermediate spectrum compared to its initial state revealing a decreased spin-spin interaction. The inter-spin distances for the BR initial state and the M intermediate are calculated to be 0.7 and 0.8 nm, respectively. The fitting also uncovered an amount of 50 % non-interacting nitroxides. This percentage results from singly spin labeled proteins and is in agreement with the determined spin label to BR ratio of 1.4-1.6. The EPR spectra of L100R1 & S226R1 (not shown) reveal an average inter-spin distance of 1.4 ± 0.1 nm for the initial state and 1.2 ± 0.1 nm for the trapped M intermediate. No inter-spin distance changes were detected for V101R1&A160R1. These results are in agreement with an outward movement of the cytoplasmic end of helix F and an inward tilt of helix G into the direction of the proton channel as shown in figure 7e.

The time course of these helix movements was resolved at room temperature by detection of the signal amplitude changes at fixed B-field positions, where the kinetic EPR difference spectrum exhibits local extremes. This is again exemplified for the double mutant V101R1&A168R1 (figure 7c). The rise of the EPR transient showing the outward movement of helix F occurs prior to the M-decay, hence, the trigger for this conformational change must be independent from the reprotonation of the Schiff Base. The recovery of the ground state conformation of helix F can be satisfactorily fitted with the two dominating relaxation time constants of the optical transient measured at 570 nm.

5.2.2. Sensory rhodopsin-transducer interaction: changes upon protein-protein interaction

On light excitation the pSRII receptor reverts to the long lived M-intermediate which was proposed to represent the signaling state (73). We have demonstrated that during this reaction helix F of the receptor moves outwardly similar to the conformational change found in BR (74). This helix movement of the receptor is transferred to the transducer as revealed by comparing the inter-residual distance changes observed between transducer / transducer as well as receptor / transducer during the photocycle (8). Low temperature experiments (T = 170 K) with the receptor trapped in the M intermediate show changes of the interaction strengths between the two TM2 and between TM2 and helix F of pSRII: Residues S158R1/K157R1 of helix F approach TM2-residues A80R1/T81R1 in M. Simultaneously, the strong dipolar interaction between the two V78R1 in neighboring TM2 helices is reduced significantly revealing a rearrangement of the two TM2 helices (see figure 5a,b).

In figure 8 the room temperature EPR signal changes recorded for V78R1 are compared with that of L159R1 which corresponds to an amino acid position on helix F oriented towards the inside of the receptor (cf. figure 5b). Additionally, an optical trace monitoring the depletion and reformation of the pSRII ground state (at 500 nm) is depicted in this figure. The kinetic difference spectra recorded at room temperature represent features of a transient increase of the inter-spin distance between V78R1 and V78R1' and of a transient mobilization for L159R1. Thus, the three signals shown in figure 8 record events occurring at the level of the retinal chromophore (500 nm optical trace), of helix F (L159R1, EPR trace), and of TM2 (V78R1, EPR trace) which allows to follow the signal transfer in the sequence retinal-helix F - TM2 and *vice versa*. It is obvious from these three traces, that the formation of the activated receptor/transducer complex is faster than the time resolution of the present EPR-device.

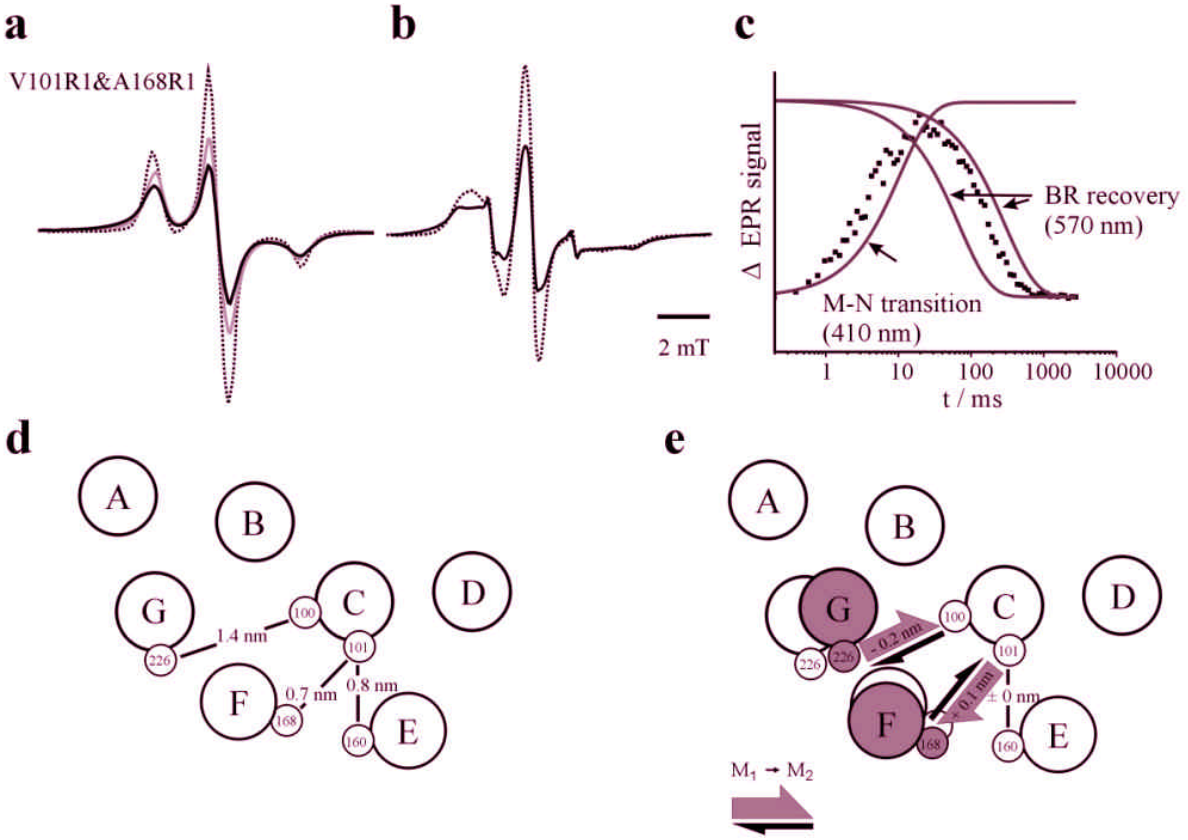

Figure 7. EPR spectra of the BR double mutant V101R1&A168R1. Pronounced dipolar broadening is observed for the initial state (black lines) as revealed by the comparison with the superposition of the spectra of the singly labeled mutants (dotted lines): (a) at 170 K and (b) at 293 K. Illumination at 220 K and fast cooling to 170 K decreases the line width for the doubly labeled mutant (gray line in (a)). All spectra are normalized to a constant spin number. (c) EPR signal changes after photo-excitation (squares). The solid gray lines show the time course of the M to N transition and two dominating rates of the recovery of the BR initial state determined by a multi-exponential fit of transients determined at 410 and 570 nm, respectively. The inter-spin distance between positions 101 and 168 increases prior to the M decay and returns into its initial value with a time course that can be fitted with the two dominating time constants of the BR initial state recovery (not shown). (d) and (e), schematic display of a top view of the cytoplasmic surface of BR with indicated inter-spin distances for the BR initial state and distance changes occurring during the photocycle. According to the distance measurements of the initial and of the M state (see text) the outward movement of the cytoplasmic terminus of helix F by 0.1 nm is accompanied by an inward shift of the cytoplasmic terminus of helix G by 0.2 nm (47).

This state remains unchanged about two orders of magnitude in time. With the reformation of the ground state, the reactions characteristic for the receptor seems to be decoupled from those of the transducer. The resetting movement of helix F into the original position seems to precede the recovery of TM2 position, the latter one being delayed by approximately a factor of 4.

6. PERSPECTIVES: SDSL STUDY OF CONFORMATIONAL CHANGES IN PROTEIN SUBSTRATES THAT AFFECT THEIR RATES OF UBIQUITINATION

The discussed features make SDSL a promising approach for the study of conformational dynamics involved in protein ubiquitination. For example, cytochrome P450 2E1 (CYP2E1) levels are elevated in response to substrates such as ethanol, and it has been postulated that substrate binding alters the conformation and dynamics of the ubiquitination target domains on CYP2E1 (12-14). Hence, it is of considerable interest to study the conformational changes of proteins such as CYP2E1 upon substrate binding with special attention to the ubiquitination target domains. The detailed understanding of the influence of substrates, therapeutic agents and inducers like isoniazid on the conformation and conformational dynamics of CYP2E1 and on its interaction with ubiquitin/ubiquitination machinery is expected to facilitate the design of new compounds of analytical as well as pharmacological importance.

The determination of conformational changes upon membrane/substrate/inhibitor binding in the vicinity of the target sites for ubiquitination would be

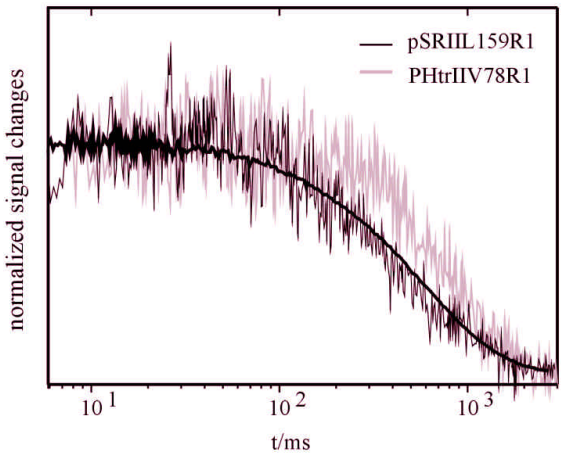

Figure 8. EPR transients (noisy lines) and the corresponding optical traces recorded at 500 nm (continuous line) of the receptor – transducer complex pSRII - pHtrV78R1 (gray trace), and of the pSRII mutant L159R1 (black trace) after activation with light. The EPR signal changes in the complex uncover a transient distance change between positions 78 of the two transmembrane helices of the transducer, TM2 and TM2' (see figure 5b), the rise of which is faster than 4 ms. The transient increase of the mobility of the spin label side chain at position 159 indicates an outward movement of helix F of the receptor (8, 74).

straightforward using an approach as described above. Nitroxide side chains may be introduced at different sites close to the putative ubiquitination domains, *i.e.*, in the sequence between positions 316 and 325 in the CYP2E1 protein (13). The accessible native cysteines have to be replaced by serines or alanines to reduce interference. EPR spectra of the free and membrane bound spin labeled protein in the presence and absence of different substrates or inhibitors (e.g. ethanol, isoniazid, acetaminophen) and ubiquitin are expected to provide information on the possible conformational changes in these regions or altered protein dynamics. The distance between singly spin labeled sites and the heme iron (catalytic site for CYP2E1) or between two spin label side chains attached to CYP2E1 can be determined through the strength of the spin-spin interaction according to the protocols discussed above. The variation of the inter-spin distance in the presence or absence of different substrates and/or ubiquitin will allow monitoring of the helix or domain movements or changes in secondary or tertiary structure. These data in combination with EPR spectra simulations on the basis of molecular dynamic simulations (section 4.2) will provide the necessary information for modeling of the changed conformations on the level of side chain orientations. Spin labels with an immobilized nitroxide side chain will additionally provide information on the flexibility of different enzyme domains and its dependence on the state of substrate and ubiquitin binding. Stopped-flow methods can be applied to follow the conformational kinetics upon addition of substrate or ubiquitin with millisecond time resolution. The results are expected to elucidate how protein conformational changes are involved in regulation of protein turnover by ubiquitination.

7. ACKNOWLEDGMENT

We gratefully acknowledge the support of the Deutsche Forschungsgemeinschaft in the frame of the Schwerpunktprogramm SPP1051 and the Sonderforschungsbereich SFB 394.

8. REFERENCES

1. Hubbell, W.L., H.S. McHaourab, C. Altenbach, and M.A. Lietzow: Watching proteins move using site-directed spin labeling. *Structure* 4, 779-783 (1996)
2. Hubbell, W.L., A. Gross, R. Langen, and M.A. Lietzow: Recent advances in site-directed spin labeling of proteins. *Curr Opin Struct Biol* 8, 649-656 (1998)
3. Hubbell, W.L., D.S. Cafiso, and C. Altenbach: Identifying conformational changes with site-directed spin labeling. *Nat Struct Biol* 7, 735-739 (2000)
4. Feix, J.B. and C.S. Klug: Site-directed spin labeling of membrane proteins and peptide-membrane interactions. In: Spin Labeling: The Next Millenium. Eds: L. Berliner. Plenum Press, New York. 251-281 (1998)
5. Koteiche, H.A. and H.S. Mchaourab: Folding pattern of the a-crystallin domain in aA-crystallin determined by site-directed spin labeling. *J Mol Biol* 294, 561-77 (1999)
6. Perozo, E., D.M. Cortes, and L.G. Cuello: Three-dimensional architecture of a K+ channel: implications for the mechanism of ion channel gating. *Nature of Structural Biology* 5, 459-469 (1998)
7. Mchaourab, H.S. and E. Perozo: Determination of protein folds and conformational dynamics using spin-labeling EPR spectroscopy. In: Distance Measurements in Biological Systems by EPR. Eds: L. Berliner, S.S. Eaton, and G.R. Eaton. Kluwer, New York (2000)
8. Wegener, A.A., J.P. Klare, M. Engelhard, and H.-J. Steinhoff: Structural insights into the early steps of receptor-transducer signal transfer in archaeal phototaxis. *EMBO J* 20, 5312-5319 (2001)
9. Lam, Y.A., T.G. Lawson, M. Velayutham, J.L. Zweier, and C.M. Pickart: A proteasomal ATPase subunit recognizes the polyubiquitin degradation signal. *Nature* 416, 763-767 (2002)
10. Finley, D.: Ubiquitin chained and crosslinked. *Nature cell biology* 4, E121-E123 (2002)
11. Hershko, A. and A. Ciechanover: The ubiquitin system. *Annu Rev Biochem* 67, 425-479 (1998)
12. Roberts, B.J., B.J. Song, Y. Soh, S.S. Park, and S.E. Shoaf: Ethanol induces CYP2E1 by protein stabilization. *J Biol Chem* 270, 29632-29635 (1995)
13. Banerjee, A., T.A. Kocarek, and R.F. Novak: Identification of a ubiquitination-target/substrate-interaction domain of cytochrome P450 (CYP)2E1. *Drug Metab Dispos* 28, 118-124 (2000)
14. Banerjee, A. and R.C. Wade: Elusive recognition determinants for ubiquitination. *J Mol Recognit* 15, 3-5 (2002)
15. Berliner, L.J., J. Grunwald, H.O. Hankovszky, and K. Hideg: A novel reversible thiol-specific spin label: papain active site labeling and inhibition. *Anal Biochem* 119, 450-455 (1982)
16. Berliner, L.J.: Spin Labeling : Theory and Applications. 1976, New York: Academic Press.

17. Berliner, L.J.: Spin Labeling II: Theory and Applications. 1979, New York: Academic Press.
18. Berliner, L.J. and J. Reuben: Biological Magnetic Resonance. Vol. VIII: Spin Labeling Theory and Applications. Eds: L.J. Berliner and J. Reuben. 1989: Plenum Press.
19. Mchaourab, H.S., M.A. Lietzow, K. Hideg, and W.L. Hubbell: Motion of spin-labeled side chains in T4 lysozyme. Correlation with protein structure and dynamics. *Biochemistry* 35, 7692-704 (1996)
20. Steinhoff, H.J. and W.L. Hubbell: Calculation of electron paramagnetic resonance spectra from Brownian dynamics trajectories: application to nitroxide side chains in proteins. *Biophys J* 71, 2201-2212 (1996)
21. Steinhoff, H.J., M. Müller, C. Beier, and M. Pfeiffer: Molecular dynamics simulation and EPR spectroscopy of nitroxide side chains in bacteriorhodopsin. *J Molecular Liquids* 84, 17-27 (2000)
22. Hubbell, W.L. and C. Altenbach: Investigation of structure and dynamics in membrane proteins using site-directed spin labeling. *Curr Opin Struct Biol* 4, 566-573 (1994)
23. Essen, L.O., R. Siegert, W.D. Lehmannn, and D. Oesterhelt: Lipid patches in membrane protein oligomers - crystal structure of the bacteriorhodopsin-lipid complex. *Proc Natl Acad Sci U S A* 95, 11673-11678 (1998)
24. Luecke, H., H.T. Richter, and J.K. Lanyi: Proton transfer pathways in bacteriorhodopsin at 2.3 angstrom resolution. *Science* 280, 1934-1937 (1998)
25. Luecke, H., B. Schobert, H.T. Richter, J.P. Cartailler, and J.K. Lanyi: Structure of bacteriorhodopsin at 1.55 angstrom resolution. *J Mol Biol* 291, 899-911 (1999)
26. Pebay-Peyroula, E., G. Rummel, J.P. Rosenbusch, and E.M. Landau: X-ray structure of bacteriorhodopsin at 2.5 angstroms from microcrystals grown in lipidic cubic phases. *Science* 277, 1676-1681 (1997)
27. Pfeiffer, M., T. Rink, K. Gerwert, D. Oesterhelt, and H.J. Steinhoff: Site-directed spin-labeling reveals the orientation of the amino acid side-chains in the E-F loop of bacteriorhodopsin. *J Mol Biol* 287, 163-171 (1999)
28. Freed, J.H.: Theory of slow tumbling ESR spectra for nitroxides. In: Spin Labeling, Theory and Application. Academic Press, New York. 53-132 (1976)
29. Barnes, J.P., Liang, Z., Mchaourab, H., Freed, J. H. and Hubbell, W. L.: A multifrequency electron resonance study of T4 lysozyme dynamics. *Biophys J* 76, 3298-3306 (1999)
30. Borbat, P.P., A.J. Costa-Filho, K.A. Earle, J.K. Moscicki, and J.H. Freed: Electron Spin Resonace in Studies of Membranes and Proteins. *Science* 291, 266-269 (2001)
31. Altenbach, C., T. Marti, H.G. Khorana, and W.L. Hubbell: Transmembrane protein structure: spin labeling of bacteriorhodopsin mutants. *Science* 248, 1088-1092 (1990)
32. Farahbakhsh, Z., C. Altenbach, and W.L. Hubbell: Spin labeled cysteines as sensors for protein-lipid interaction and conformation in rhodopsin. *Photochem Photobiol* 56, 1019-1033 (1992)
33. Altenbach, C., D.A. Greenhalgh, H.G. Khorana, and W.L. Hubbell: A collision gradient method to determine the immersion depth of nitroxides in lipid bilayers: application to spin-labeled mutants of bacteriorhodopsin. *Proc Natl Acad Sci U S A* 91, 1667-1671 (1994)
34. Burghaus, O., M. Rohrer, T. Gotzinger, M. Plato, and K. Möbius: A novel high-field/high-frequency EPR and ENDOR spectrometer operating at 3 mm wavelength. *Measurement Science & Technology* 3, 765-774 (1992)
35. Prisner, T.F., A. Vanderest, R. Bittl, W. Lubitz, D. Stehlik, and K. Möbius: Time-Resolved W-Band (95 Ghz) Epr Spectroscopy of Zn-Substituted Reaction Centers of Rhodobacter Sphaeroides R-26. *Chem Phys* 194, 361-370 (1995)
36. Huber, M. and J.T. Törring: High-field EPR on the primary electron donor cation radical in single crystals of heterodimer mutant reaction centers of photosynthetic bacteria - first characterization of the G-tensor. *Chem Phys* 194, 379-385 (1995)
37. Stone, A.J.: Gauge invariance of the g tensor. *Proc Roy Soc London* A271, 424-434 (1963)
38. Steinhoff, H.J., K. Lieutenant, and J. Schlitter: Residual motion of hemoglobin-bound spin labels as a probe for protein dynamics. *Z Naturforsch* 44c, 38-46 (1989)
39. Steinhoff, H.-J., A. Savitski, C. Wegener, M. Pfeiffer, M. Plato, and K. Möbius: High-field EPR studies of the structure and conformational changes of site-directed spin labeled bacteriorhodopsin. *Biochim Biophys Acta* 1457, 253-262 (2000)
40. Hustedt, E.J. and A.H. Beth: Nitroxide spin-spin interactions: applications to protein structure and dynamics. *Annu Rev Biophys Biomol Struct* 28, 129-153 (1999)
41. Eaton, G.R., S.S. Eaton, and L.J. Berliner: Distance Measurements in Biological Systems. 2000. New York: Kluwer.
42. Hustedt, E.J., A.I. Smirnov, C.F. Laub, C.E. Cobb, and A.H. Beth: Molecular distances from dipolar coupled spin-labels - the global analysis of multifrequency continuous wave electron paramagnetic resonance data. *Biophys J* 72, 1861-1877 (1997)
43. Steinhoff, H.-J., O. Dombrowsky, C. Karim, and C. Schneiderhahn: Two dimensional diffusion of small molecules on protein surfaces: an EPR study of the restricted translational diffusion of protein-bound spin labels. *Eur Biophys J* 20, 293-303 (1991)
44. Rabenstein, M.D. and Y.K. Shin: Determination of the distance between two spin labels attached to a macromolecule. *Proc Natl Acad Sci USA* 92, 8239-8243 (1995)
45. Steinhoff, H.J., N. Radzwill, W. Thevis, V. Lenz, D. Brandenburg, A. Antson, G. Dodson, and A. Wollmer: Determination of interspin distances between spin labels attached to insulin: comparison of electron paramagnetic resonance data with the X- ray structure. *Biophys J* 73, 3287-3298 (1997)
46. Altenbach, C., K.J. Oh, R.J. Trabanino, K. Hideg, and W.L. Hubbell: Estimation of inter-residue distances in spin labeled proteins at physiological temperatures: experimental strategies and practical limitations. *Biochemistry* 40, 15471-82 (2001)
47. Radzwill, N., K. Gerwert, and H.-J. Steinhoff: Time-resolved detection of transient movement of helices F and G in doubly spin-labeled bacteriorhodopsin. *Biophys J* 80, 2856-2866 (2001)
48. Closs, G.L., M.D.E. Forbes, and P. Piotrowiak: Spin and reaction dynamics in flexible polymethylene biradicals as studied by EPR, NMR, and optical spectroscopy and

magnetic field effect. Measurements and mechanisms of scalar electron spin-spin coupling. *J Am Chem Soc* 114, 3285-3294 (1992)
49. Fiori, W.R. and G.L. Millhauser: Exploring the peptide 3(10)-helix reversible alpha-helix equilibrium with double label electron spin resonance. *Biopolymers* 37, 243-250 (1995)
50. Borbat, P.P. and J.H. Freed: Multi-quantum ESR and distance measurements. *Chem Phys Lett* 313, 145-154 (1999)
51. Pannier, M., S. Veit, A. Godt, G. Jeschke, and H.W. Spiess Dead-Time Free Measurement of Dipole-Dipole Interactions between Electron Spins. *J Magn Reson* 142, 331-340 (2000)
52. Cai, K.W., R. Langen, W.L. Hubbell, and H.G. Khorana: Structure and Function in Rhodopsin - Topology of the C-Terminal Polypeptide Chain in Relation to the Cytoplasmic Loops. *Proc Natl Acad Sci USA* 94, 14267-14272 (1997)
53. Altenbach, C., K. Yang, D.L. Farrens, Z.T. Farahbakhsh, H.G. Khorana, and W.L. Hubbell: Structural features and light-dependent changes in the cytoplasmic interhelical E-F loop region of rhodopsin - a site-directed spin-labeling study. *Biochemistry* 35, 12470-12478 (1996)
54. Gross, A., L. Columbus, K. Hideg, C. Altenbach, and W.L. Hubbell: *Biochemistry* 38, 10324-10335 (1999)
55. Voss, J., W.L. Hubbell, and H.R. Kaback: Helix Packing in the Lactose Permease Determined By Metal-Nitroxide Interaction. *Biochemistry* 37, 211-216 (1998)
56. Koteiche, H.A., A.R. Berengian, and H.S. Mchaourab: Identification of protein folding patterns using site-directed spin labeling. Structural characterization of a beta-sheet and putative substrate binding regions in the conserved domain of a A-crystallin. *Biochemistry* 37, 12681-8 (1998)
57. Farrens, D.L., C. Altenbach, K. Yang, W.L. Hubbell, and H.G. Khorana: Requirement of rigid-body motion of transmembrane helices for light activation of rhodopsin. *Science* 274, 768-770 (1996)
58. Tiebel, B., N. Radzwill, L.M. Aung-Hilbrich, V. Helbl, H.J. Steinhoff, and W. Hillen: Domain motions accompanying Tet repressor induction defined by changes of interspin distances at selectively labeled sites. *J Mol Biol* 290, 229-240 (1999)
59. Perozo, E., D.M. Cortes, and L.G. Cuello: Structural rearrangement underlying K^+-channel activation gating. *Science* 285, 73-78 (1999)
60. Leigh, J.S.: ESR rigid lattice line shape in a system of two interacting spins. *J Chem Phys* 52, 2608-2612 (1970)
61. Voss, J., L. Salwinski, H.R. Kaback, and W.L. Hubbell: A method for distance determination in proteins using a designed metal ion binding site and site-directed spin labeling - evaluation with T4 lysozyme. *Proc Natl Acad Sci USA* 92, 12295-12299 (1995)
62. Voss, J., W.L. Hubbell, and H.R. Kaback: Distance determination in proteins using designed metal ion binding sites and site-directed spin labeling - application to the lactose permease of escherichia coli. *Proc Natl Acad Sci USA* 92, 12300-12303 (1995)
63. Farahbakhsh, Z., K. Hideg, and W.L. Hubbell: Photoactivated conformational changes in rhodopsin: a time resolved spin label study. *Science* 262, 1416-1420 (1993)
64. Steinhoff, H.J., R. Mollaaghababa, C. Altenbach, K. Hideg, M. Krebs, H.G. Khorana, and W.L. Hubbell: Time-resolved detection of structural changes during the photocycle of spin-labeled bacteriorhodopsin. *Science* 266, 105-107 (1994)
65. Thorgeirsson, T.E., W.Z. Xiao, L.S. Brown, R. Needleman, J.K. Lanyi, and Y.K. Shin: Transient channel-opening in bacteriorhodopsin - an EPR study. *J Mol Biol* 273, 951-957 (1997)
66. Xiao, W., L.S. Brown, R. Needleman, J.K. Lanyi, and Y.-K. Shin: Light-induced rotation of a transmembrane alpha-helix in bacteriorhodopsin. *J Mol Biol* 304, 715-721 (2000)
67. Shin, Y., C. Levinthal, F. Levinthal, and W.L. Hubbell: Colicin E1 binding to membranes: time resolved studies of spin-labeled mutants. *Science* 259, 960-963 (1993)
68. Elove, G.A., A.K. Bhuyan, and H. Roder: Kinetik mechanism of cytochrome c folding: involvement of the heme and its ligands. *Biochemistry* 33 (1994)
69. DeWeerd, K., V. Grigoryants, Y. Sun, J.S. Fetrow, and C.P. Scholes: EPR-detected folding kinetics of externally located cysteine-directed spin-labeled mutants of iso-1-cytochrome c. *Biochemistry* 40, 15846-55 (2001)
70. Rink, T., J. Riesle, D. Oesterhelt, K. Gerwert, and H.J. Steinhoff: Spin-labeling studies of the conformational changes in the vicinity of D36, D38, T46, and E161 of bacteriorhodopsin during the photocycle. *Biophys J* 73, 983-993 (1997)
71. Mollaaghababa, R., H.J. Steinhoff, W.L. Hubbell, and H.G. Khorana: Time-resolved site-directed spin-labeling studies of bacteriorhodopsin: loop-specific conformational changes in M. *Biochemistry* 39, 1120-1127 (2000)
72. Rink, T., M. Pfeiffer, D. Oesterhelt, K. Gerwert, and H.J. Steinhoff: Unraveling photoexcited conformational changes of bacteriorhodopsin by time resolved electron paramagnetic resonance spectroscopy. *Biophys J* 78, 1519-1530 (2000)
73. Yan, B., T. Takahashi, R. Johnson, and J.L. Spudich: Identification of signaling states of a sensory receptor by modulation of lifetimes of stimulus-induced conformations: the case of sensory rhodopsin II. *Biochemistry* 30, 10686-92 (1991)
74. Wegener, A.A., I. Chizhov, M. Engelhard, and H.J. Steinhoff: Time-resolved Detection of Transient Movement of Helix F in Spin-labelled Pharaonis Sensory Rhodopsin II. *J Mol Biol* 301, 881-891 (2000)
75. Wegener, C., A. Savitsky, M. Pfeiffer, K. Möbius, and H.-J. Steinhoff: High-field EPR-detected shifts of magnetic tensor components of spin label side chains reveal protein conformational changes: the proton entrance channel of bacteriorhodopsin. *Applied Magnetic Resonance* 21, 441-452 (2001)

Key Words: Ubiquitin, EPR, Site-Directed Spin Labeling, Inter-Spin Distance, Cytochrome P450, Protein-Protein Interaction, Review

Send correspondence to: Prof. Dr. Heinz-Jürgen Steinhoff, University Osnabrueck, Department of Physics, Barbarastrasse 7, 49069 Osnabrueck, Germany, Tel.: +49 541-969-2664, Fax: +49-541-969-2656, E-mail: hsteinho@uni-osnabrueck.de